

See discussions, stats, and author profiles for this publication at: <https://www.researchgate.net/publication/12877040>

Cyanide Binding to *Lucina pectinata* Hemoglobin I and to Sperm Whale Myoglobin: An X-Ray Crystallographic Study

ARTICLE in BIOPHYSICAL JOURNAL · SEPTEMBER 1999

Impact Factor: 3.97 · DOI: 10.1016/S0006-3495(99)76959-6 · Source: PubMed

CITATIONS

57

READS

37

8 AUTHORS, INCLUDING:



Martino Bognesi

University of Milan

478 PUBLICATIONS 12,745 CITATIONS

SEE PROFILE



Camillo Rosano

Azienda Ospedaliera Universitaria San Marti...

101 PUBLICATIONS 1,592 CITATIONS

SEE PROFILE



Menico Rizzi

Amedeo Avogadro University of Eastern Pie...

98 PUBLICATIONS 2,871 CITATIONS

SEE PROFILE



Jonathan B Wittenberg

Albert Einstein College of Medicine

106 PUBLICATIONS 5,521 CITATIONS

SEE PROFILE

Cyanide Binding to *Lucina pectinata* Hemoglobin I and to Sperm Whale Myoglobin: An X-Ray Crystallographic Study

Martino Bolognesi,*[#] Camillo Rosano,* Romeo Losso,* Alberto Borassi,* Menico Rizzi,[#]
Jonathan B. Wittenberg,[¶] Alberto Boffi,^{||} and Paolo Ascenzi*^{**}

*Dipartimento di Fisica-INFM, Università di Genova, and Centro Biotecnologie Avanzate-IST, I-16132 Genova, Italy; [#]Dipartimento di Genetica e Microbiologia, Università di Pavia, I-27100 Pavia, Italy; [§]Dipartimento di Scienze Mediche, Università del Piemonte Orientale "A. Avogadro," I-28100 Novara, Italy; [¶]Department of Physiology and Biophysics, Albert Einstein College of Medicine, Bronx, New York 10461 USA; ^{||}Centro di Biologia Molecolare-CNR, and Dipartimento di Scienze Biochimiche "A. Rossi Fanelli," Università di Roma "La Sapienza," I-00185 Rome, Italy; and ^{**}Dipartimento di Biologia, Università di Roma "Tre," I-00146 Rome, Italy

ABSTRACT The x-ray crystal structures of the cyanide derivative of *Lucina pectinata* monomeric hemoglobin I (*L. pectinata* HbI) and sperm whale (*Physeter catodon*) myoglobin (Mb), generally taken as reference models for monomeric hemoproteins carrying hydrogen sulfide and oxygen, respectively, have been determined at 1.9 Å (*R*-factor = 0.184), and 1.8 Å (*R*-factor = 0.181) resolution, respectively, at room temperature ($\lambda = 1.542$ Å). Moreover, the x-ray crystal structure of the *L. pectinata* HbI:cyanide derivative has been studied at 1.4-Å resolution (*R*-factor = 0.118) and 100 K (on a synchrotron source $\lambda = 0.998$ Å). At room temperature, the cyanide ligand is roughly parallel to the heme plane of *L. pectinata* HbI, being located ~ 2.5 Å from the iron atom. On the other hand, the crystal structure of the *L. pectinata* HbI:cyanide derivative at 100 K shows that the diatomic ligand is coordinated to the iron atom in an orientation almost perpendicular to the heme (the Fe-C distance being 1.95 Å), adopting a coordination geometry strictly reminiscent of that observed in sperm whale Mb, at room temperature. The unusual cyanide distal site orientation observed in *L. pectinata* HbI, at room temperature, may reflect reduction of the heme Fe(III) atom induced by free radical species during x-ray data collection using Cu K α radiation.

INTRODUCTION

Lucina pectinata hemoglobin I (*L. pectinata* HbI) and sperm whale (*Physeter catodon*) myoglobin (Mb) are generally taken as the prototype models for monomeric hemoproteins carrying hydrogen sulfide and oxygen, respectively (see Springer et al., 1994; Bolognesi et al., 1997). The bivalve mollusc *L. pectinata*, living in sulfide-rich coastal sediments, houses chemoautotrophic symbiotic bacteria that couple the energy released by the oxidation of the environmental hydrogen sulfide to the fixation of carbon dioxide into hexoses, which are the only source of carbon for the mollusc. The biological function of hemoglobin I, II, and III (HbI, HbII, and HbIII, respectively), located in the cytoplasm of the mollusc bacteriocyte gill cells, is related to the transport of hydrogen sulfide and oxygen, respectively, from the external environment to the symbiotic bacteria (see Kraus and Wittenberg, 1990; Kraus et al., 1990; Wittenberg and Wittenberg, 1990; Rizzi et al., 1994, 1996; Bolognesi et al., 1997). Conversely, sperm whale Mb facilitates oxygen transport from circulating hemoglobin (Hb) to the mitochondria and acts as the O₂ reservoir during diving. Oxygen release from the binary sperm whale Mb:O₂ adduct is modulated by lactate, which acts as an allosteric effector (see Springer et al., 1994; Giardina et al., 1996).

Under physiological conditions, i.e., in the presence of both oxygen and hydrogen sulfide, the Fe(II) heme iron atom of ferrous monomeric *L. pectinata* HbI is readily oxidized to Fe(III), with the concomitant formation of the heme Fe(III):hydrogen sulfide adduct. The affinity of hydrogen sulfide for ferric *L. pectinata* HbI ($K = 2.9 \times 10^8$ M⁻¹, at pH 7.5 and 20.0°C) is ~ 5000 -fold higher than that observed for ferric *L. pectinata* HbII and HbIII, as well as for ferric sperm whale Mb, mainly resulting from slower ligand dissociation. Hydrogen sulfide is released from ferric *L. pectinata* HbI upon reduction of the heme iron atom. In ferric *L. pectinata* HbI, the heme iron-bound hydrogen sulfide is stabilized by hydrogen bonding with Gln(64)E7, and by aromatic-electrostatic interactions with residues Phe(29)B10, Phe(43)CD1, and Phe(68)E11, forming the so-called Phe-cage. (Amino acid residues have been identified by their three-letter code, their sequence number, within parentheses, and their topological position, within the helices of the globin fold (Perutz, 1979). For the numbering of the heme group atoms, the scheme of Takano (1977) has been adopted.) The much lower affinity of hydrogen sulfide for ferric *L. pectinata* HbII and HbIII may be related to the perturbation(s) brought about in the ligand-binding pocket by the OH group of Tyr(29)B10, which alters the size and polarity of the distal "Phe-cage," hampering its action in hydrogen sulfide stabilization. In a comparable way, sperm whale Mb residues at positions E7, B10, and E11 (His(64), Leu(29), and Val(68), respectively) modify the size and the polarity of the heme distal site, rendering hydrogen sulfide binding to the iron atom thermodynamically unfavorable (see Kraus and Wittenberg, 1990; Kraus et al., 1990; Wittenberg and Wittenberg, 1990;

Received for publication 3 December 1998 and in final form 30 April 1999.

Address reprint requests to Dr. Martino Bolognesi, Centro Biotecnologie Avanzate, Università di Genova, Largo R. Benzi 10, I-16132 Genova, Italy. Tel.: +39-010-5737306; Fax: +39-010-5737306; E-mail: bolognesi@fisica.unige.it.

© 1999 by the Biophysical Society

0006-3495/99/08/1093/07 \$2.00

Rizzi et al., 1994, 1996; Bolognesi et al., 1997; Nguyen et al., 1998).

L. pectinata HbI, HbII, and HbIII, as well as sperm whale Mb, bind oxygen with similar affinity ($K \approx 2.5 \times 10^6 \text{ M}^{-1}$, at pH 7.5 and 20.0°C). However, different stabilization modes of the heme iron-bound ligand occur in ferrous *L. pectinata* HbI, HbII, and HbIII, as well as in sperm whale Mb, as suggested by the very different values of the kinetic parameters for the formation and dissociation of the heme iron:O₂ complexes. In *L. pectinata* HbI, the heme iron-bound O₂ may be stabilized in a fashion similar to that reported for hydrogen sulfide, i.e., by interaction with Gln(64)E7 and the "Phe-cage." In *L. pectinata* HbII and HbIII, the heme iron-bound dioxygen may be stabilized by hydrogen bonds to TyrB10 and GlnE7 residues, as reported for *Ascaris suum* and *Parascaris equorum* Hb. Furthermore, in sperm whale Mb, the heme iron-bound O₂ is stabilized by a hydrogen bond to the distal His(64)E7 residue (see Kraus and Wittenberg, 1990; Kraus et al., 1990; Wittenberg and Wittenberg, 1990; Springer et al., 1994; Rizzi et al., 1994, 1996; Giardina et al., 1996; Bolognesi et al., 1997).

To address the question of diatomic ligand recognition by hemoproteins displaying quite different heme distal sites and reactivity, the x-ray crystal structures of the cyanide derivative of *L. pectinata* HbI and of sperm whale Mb have been determined at room temperature (Cu K α radiation), at 1.9-Å and 1.8-Å resolution (*R*-factor = 0.184, and 0.181, respectively). Moreover, for *L. pectinata* HbI:cyanide complex, the crystallographic analysis has been extended to 1.4-Å resolution (on a synchrotron source, *R*-factor = 0.118) at 100 K. The present results have been analyzed in parallel with those of monomeric (non)vertebrate hemoglobin:cyanide derivatives.

MATERIALS AND METHODS

Ferric *L. pectinata* HbI was prepared according to the method of Kraus and Wittenberg (1990). Ferric sperm whale Mb was purified from the hemoprotein commercial preparations (from Sigma Chemical Co., St. Louis, MO), as previously reported (Lionetti et al., 1991). All chemicals (from Merck AG, Darmstadt, Germany, and Sigma Chemical Co.) were of analytical grade and were used without further purification.

Crystals of ferric *L. pectinata* HbI (monoclinic space group: P2₁; cell constants: $a = 50.7 \text{ Å}$, $b = 38.8 \text{ Å}$, $c = 42.5 \text{ Å}$, $\beta = 106.9^\circ$, at room temperature; $a = 49.4 \text{ Å}$, $b = 37.9 \text{ Å}$, $c = 41.4 \text{ Å}$, $\beta = 106.2^\circ$, at 100 K) and of sperm whale Mb (monoclinic space group: P2₁; cell constants: $a = 64.9 \text{ Å}$, $b = 31.0 \text{ Å}$, $c = 35.3 \text{ Å}$, $\beta = 105.6^\circ$) were grown from ammonium sulfate solutions, as previously described (Lionetti et al., 1991; Rizzi et al., 1994). Ferric *L. pectinata* HbI:cyanide and sperm whale Mb:cyanide complexes were obtained by soaking the aquo-met crystals in their mother liquor containing saturating concentrations of the ligand, at pH 7.0 and room temperature; the soaking time was 12 h.

X-ray diffraction data were collected, at room temperature, on a Rigaku R-axis II image plate system, coupled to a Rigaku RU200-HB rotating anode generator. Processing of the diffracted intensities was conducted using MOSFLM (Leslie, 1992) and programs from the CCP4 suite (CCP4, 1994). For x-ray data collection at 100 K, *L. pectinata* HbI:cyanide complex crystals were transferred to a solution containing 3.0 M ammonium sulfate, 30% glycerol, 0.02 M phosphate buffer, pH 6.5, as cryoprotectant. Diffracted intensities were measured at the EMBL Hamburg Outstation c/o DESY on beamline BW7A ($\lambda = 0.998 \text{ Å}$) and processed as described above (see Table 1).

The refinement of the cyanide derivative of *L. pectinata* HbI and sperm whale Mb (data at room temperature) was conducted through crystallographic restrained refinement procedures (Tronrud et al., 1987), alternated to model building/inspection based on the "O" program package (Jones et al., 1991). For the *L. pectinata* HbI:cyanide complex, the starting atomic coordinates used for phase calculation were those of Rizzi et al. (1994), referring to the aquo-met derivative, with residue substitutions as described in the Results and Discussion. The atomic coordinates of Lionetti et al. (1991), referring to the imidazole derivative, were used for the sperm whale Mb:cyanide complex.

TABLE 1 Data collection and crystallographic refinement statistics for the cyanide derivatives of *L. pectinata* HbI and sperm whale Mb

	<i>L. pectinata</i> HbI (room temperature)	<i>L. pectinata</i> HbI (100 K)	Sperm whale Mb (room temperature)
Resolution range (Å)	24.0–1.9	8.0–1.4	15.3–1.8
Completeness of data set	93.3%	92.3%	97.0%
Rmerge (%)	5.4	5.1	4.5
I/ σ (outer shell)	5.1 (2.0–1.9 Å)	4.6 (1.45–1.43 Å)	4.8 (1.9–1.8 Å)
Redundancy	4.1	3.0	3.9
Unique reflections	12,085	25,336	12,583
No. of active protein and heme atoms	1081	1103	1261
No. of solvent, cyanide and other ligand species atoms	81	204	68, 1 SO ₄ ²⁻
Average <i>B</i> -factors (Å ²)			
Main chain	30.4	7.1	40.5
Side chain	36.1	10.2	46.5
Solvent	51.2	23.3	57.5
Residues in most favored region of Ramachandran plot	96.7%	91.1%	92.5%
Residues in additional allowed regions of Ramachandran plot	3.3%	8.9%	7.5%
r.m.s. deviations			
bond lengths (Å)	0.015	0.019	0.014
bond angles (°)	2.40	2.59	2.75
planar groups (Å)	0.011	0.019	0.014
<i>B</i> -factor correlation (Å ²)	2.32	2.90	3.38
<i>R</i> -factor (all data)	0.184	0.119	0.181

For both *L. pectinata* HbI:cyanide and sperm whale Mb:cyanide derivatives studied at room temperature, the heme distal ligand and the ordered water molecules were omitted from model coordinates before the initial phase calculations and refinement. Solvent molecules were added to the atomic coordinates sets only after extensive positional and *B*-factor refinement had been run (*R*-factor ≈ 0.23 for both complexes). The cyanide ligand was fitted to its electron density only in the very final stages of the refinement. Tight stereochemical restraints were first applied to the ligand coordination geometry and subsequently released, since systematic deviations of the refined ligand from the expected stereochemistry were observed. No restraint was imposed on the Fe-C-N angle, whereas the Fe-C coordination bond was restrained to 2.2 ± 0.4 Å. The covalent C-N bond length was restrained to 1.14 ± 0.08 Å in the *L. pectinata* HbI:ligand adduct refinement (data at room temperature). On the other hand, considering that the C-N bond length in the sperm whale Mb:cyanide complex consistently showed smaller values during the refinement, it was restrained to 1.06 ± 0.08 Å. The two values adopted reflect C-N bond lengths observed for the CN^- and HCN species, respectively, in model compounds (Jones et al., 1988; Orpen et al., 1989).

The refinement of the 1.4-Å-resolution data of *L. pectinata* HbI (at 100 K) was performed starting from the refined atomic coordinates of the HbI:cyanide complex at room temperature. After atomic coordinates and isotropic *B*-factor refinement (using the TNT package; Tronrud et al. 1987) reached convergence (in the absence of ligand; *R*-factor = 0.157 at 1.4-Å resolution), individual anisotropic *B*-factors and atomic coordinates were refined using the SHELX program package (Sheldrick and Schneider, 1997). In the final refinement cycles, the cyanide ligand was fitted to electron density in the distal site and refined without any stereochemical restraint.

The atomic coordinates and structure factors for *L. pectinata* HbI:cyanide and the sperm whale Mb:cyanide complexes have been deposited with the Brookhaven Protein Data Bank, from which copies are available [as data sets: *L. pectinata* HbI (at room temperature), 1ebt; *L. pectinata* HbI (at 100 K), 1b0b; and sperm whale Mb (at room temperature), 1ebc (Abola et al., 1997)].

RESULTS AND DISCUSSION

The crystal structure of the cyanide derivative of *L. pectinata* HbI (data at room temperature) has been refined to an *R*-factor of 0.184, at 1.9-Å resolution, with ideal overall stereochemical parameters (see Table 1). The rms coordinate error estimated for the sigma-A plot is 0.21 Å (Read, 1986). A view of the *L. pectinata* HbI distal site, in the presence of the cyanide ligand, is shown in Fig. 1 A, together with the ligand electron density. The average *B*-factor for protein atoms is 32.9 Å² (30.4 Å² for backbone and 36.1 Å² for side-chain atoms, respectively) and 51.2 Å² for solvent atoms, whereas the ligand displays *B*-factors of 25.1 Å² and 38.9 Å² for the C and N atoms, respectively. The cyanide diatomic ligand is parallel to the heme plane, at a distance of ~ 2.5 Å, oriented approximately along the line connecting the methinic bridge CHB and CHD atoms. The C-N covalent bond length observed in the refined structure is 1.21 Å, and the Fe-C distance is 2.54 Å (see Table 2). The orientation of the diatomic ligand in the distal pocket of *L. pectinata* HbI is essentially dictated by contacts to the distal-site "Phe-cage" residues Phe(29)B10 (3.96 Å), Phe(43)CD1 (3.31 Å), and Phe(68)E11 (3.93 Å). Moreover, a hydrogen bond between the cyanide N atom and Gln(64)E7 OE1 atom (3.05 Å) is observed. As a result of such distal-site interactions, the ligand is completely solvent inaccessible, as defined by a 1.4-Å-radius probe.

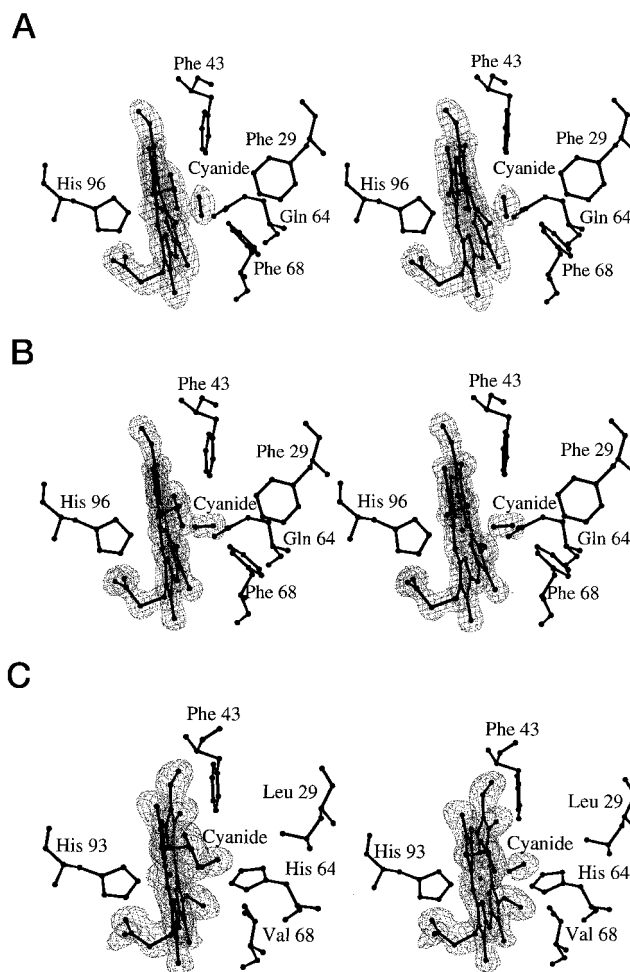


FIGURE 1 Stereo view of the heme distal site of the cyanide derivative of *L. pectinata* HbI at room temperature (A) and at 100 K (B), as well as of sperm whale Mb at room temperature (C). In the three figures the heme plane is approximately edge on, and the E helix is on the right-hand side. Electron density for the ligand (2Fo-Fc map, contoured at 1σ level) has been displayed together with the distal site residues, which are neighboring the bound cyanide. The figure was drawn with MOLSCRIPT (Kraulis, 1991).

The orientation of the ligand, parallel to the heme plane, is totally unexpected, as compared to coordination model compounds and hemoglobin:cyanide complexes (see Table 2). Concerning the location of the cyanide ligand with respect to the heme iron (the latter being contained within the porphyrin pyrrole N atoms plane), it should be noted that the Fe-N-C and the Fe-C-N angles are approximately equal ($\sim 80^\circ$), the measured Fe-C(cyanide) and Fe-N(cyanide) distances being 2.54 Å and 2.64 Å, respectively. Moreover, the perpendicular to the heme plane, passing through the Fe atom, almost bisects the C-N covalent bond. Allowing for the obvious structural differences, the cyanide location in the *L. pectinata* HbI distal site is reminiscent of that observed for the photodissociated CO molecule in ferrous sperm whale Mb (Teng et al., 1994; Schlichting et al., 1994).

The crystal structure of *L. pectinata* HbI cyanide derivative at 100 K has been refined to a *R*-factor value of 0.119,

TABLE 2 Heme iron and ligand coordination geometry observed in (non)vertebrate monomeric hemoglobin:cyanide complexes

Hemoprotein	PDB ID	<i>L. luteus</i>		<i>C.t.thummi</i>		<i>A. limacina</i>		<i>P. marinus</i>		<i>C. caretta</i>		<i>L. pectinata</i>		Sperm whale		Sperm whale		Sperm whale		Elephant	
		Hb (1)	2LH3	Ery (2)	1ECN	Mb (3)	2FAL	Hb (4)	2LHB	Mb (5)	1LHT	HbI (room temperature) (6)	1B0B	Mb (6)	1EBC	Mb (7)	2CMM	Mb (8)	1IOP	Mb (9)	1YMC
Resolution (Å)		2.0		1.4		1.9		2.0		2.0		1.9	1.4	1.8		1.8		1.9		2.0	
R factor (%)		#		#		15.1		14.2		17.8		18.4	11.8	18.1		18.7		19.5		12.9	
Average Fe—N (heme) distance (Å)		2.15		2.04		1.96		2.01		1.93		1.98	2.02	2.03		2.00		1.96		2.04	
Fe—His F8 (NE2) distance (Å)		2.18		2.12		2.12		2.10		2.15		2.15	2.13	2.02		2.21		2.02		2.14	
Fe—CN (C) distance (Å)		2.28		2.19		2.15		1.89		2.35		2.54	1.95	2.02		1.92		1.89		2.12	
Fe—CN (N) distance (Å)		3.25		3.32		2.85		2.99		2.82		2.64	3.09	3.06		2.90		3.11		2.99	
C—N (CN) distance (Å)		1.09		1.16		1.14		1.19		1.15		1.21	1.15	1.06		1.31		1.25		1.06	
E7—CN (N) distance (Å) [§]		2.80		3.93		2.91		3.09		3.01		3.05	3.05	2.68		3.58		2.66		2.90	
Fe—C—N angle (°)		148		165		116		150		102		81	178	166		127		165		137	

(1) Kuranova et al. (1982).
(2) Steigemann and Weber (1979).
(3) Conti et al. (1993).
(4) Honzatko et al. (1985).
(5) Nardini et al. (1995).
(6) Present study.
(7) 5,10,15,20-Tetramethylporphyrin-substituted sperm whale Mb; Neyra et al. (1993).
(8) 6,7-Dicarboxy-1,2,3,4,5,8-hexamethylheme-substituted sperm whale Mb; Neyra et al. (1998).
(9) Horse sulfMb C; Evans et al. (1994).
(10) Bisig et al. (1995).
[§]R-factor value not available.

[§]Residue E7 is Gln in *L. pectinata* HbI and elephant Mb, His in *L. luteus* Hb, *C.t.thummi* Ery, *P. marinus* Hb, *C. caretta* Mb, sperm whale Mb and horse Mb, and Val in *A. limacina* Mb.

with ideal overall stereochemistry (see Table 1). Besides the 1091 protein atoms and the 202 located water molecules, the refined model includes alternative conformations for eight side chains (Lys(11)A9, Ser(12)A10, Ser(13)A11, Lys(16)A14, Ser(18)A16, Lys(42)C7, and Val(76)E19). The average *B*-factor for the protein atoms is 8.5 \AA^2 (7.1 \AA^2 for main-chain and 10.2 \AA^2 for side-chain atoms, respectively), whereas the average solvent *B*-factor is 23.3 \AA^2 . The cyanide ligand displays *B*-factors of 4.8 \AA^2 and 7.2 \AA^2 for the C and N atoms, respectively. The estimate rms coordinate error is 0.07 \AA (Read, 1986).

At 100 K (see Fig. 1 B), the cyanide ligand is coordinated to the heme iron of *L. pectinata* HbI, with an orientation approximately perpendicular to the porphyrin plane. The Fe-C-N angle is 177° , and the Fe-C coordination bond is virtually coincident with the heme normal. The Fe-C distance (1.95 \AA ; see Table 2) is compatible with a full coordination bond between the two atomic species, the C-N bond length being 1.15 \AA . No significant deviation of the Fe atom from the porphyrin pyrrole N atoms plane is observed. The cyanide is in contact with the "Phe-cage" residues Phe(29)B10 (3.28 \AA), Phe(43)CD1 (3.60 \AA), and Phe(68)E11 (3.80 \AA), whereas the ligand N atom is hydrogen bonded to the Gln(64)E7 OE2 atom (3.00 \AA). Moreover, the cyanide is fully inaccessible to solvent.

The overall *L. pectinata* HbI three-dimensional structures, studied at room and cryotemperatures, are in strict agreement. The r.m.s.d. calculated over the whole $\text{C}\alpha$ chains (at the two temperatures) is 0.33 \AA , reflecting minor modifications in the crystal packing contacts induced by unit cell contraction upon freezing. The refinement of *L. pectinata* HbI at high resolution has allowed a verification of the amino acid sequence proposed by Rizzi et al. (1994), on the basis of partial peptide sequence analysis and the aquo-met protein structure there reported. Indeed, corrections to five amino acid locations were deemed necessary, based on the $1.4\text{-}\text{\AA}$ refined model. The modified residues are Glu(3)A1 \rightarrow Ser, Thr(11)A9 \rightarrow Lys, Ser(114)G13 \rightarrow Ala, Glu(137)H18 \rightarrow Met, and Glu(139)H20 \rightarrow Arg. Moreover, the N-terminal residue (Ser(1)) was found to be acetylated. The amended amino acid sequence was adopted in both *L. pectinata* HbI:cyanide complex refinement processes here reported.

The sperm whale Mb:cyanide complex was refined to an *R*-factor value of 0.181 (at room temperature) with good overall stereochemistry (see Table 1). The heme Fe-C(cyanide) coordination distance is 2.02 \AA , and the Fe-C-N angle is 166° , the Fe atom being in plane with respect to the porphyrin pyrrole N atoms. The ligand orientation is almost perpendicular to the heme plane (see Fig. 1 C), the Fe-C bond deviating by $\sim 10^\circ$ from the heme normal. The rms coordinate error estimated from the sigma-A plot is 0.21 \AA (Read, 1986). The average *B*-factor for the protein atoms is 43.4 \AA^2 (40.5 \AA^2 for main-chain and 46.5 \AA^2 for side-chain atoms, respectively), and the average solvent *B*-factor is 57.6 \AA^2 , whereas the cyanide ligand displays *B*-factors of 42.4 \AA^2 and 45.5 \AA^2 for the C and N atoms, respectively.

The C-N covalent bond length observed in the refined structure is 1.06 \AA .

In sperm whale Mb, the cyanide ligand is in contact with Phe(43)CD1 (3.63 \AA) and Val(68)E11 (3.35 \AA), essentially through the N atom, which, in turn, is hydrogen bonded to the His(64)E7 NE2 atom (2.68 \AA) (see Table 2). His(64)E7 locks the ligand in the distal site and makes it fully inaccessible to solvent. Indeed, besides cyanide, no residual electron density (indicative of buried water molecule(s)) is present in the heme distal site. Thus the overall cyanide-binding mode to the heme iron of sperm whale Mb is in agreement with what has been observed for cyanide complexes of monomeric (non)vertebrate hemoglobins (see Table 2), human Hb (Paoli et al., 1997), nitrophorin-1 (Weichsel et al., 1998), and peroxidase from *Arthromyces ramosus* (Fukuyama et al., 1995).

Comparison of the sperm whale Mb:cyanide complex structure (here described) with that of the same adduct in 6,7-dicarboxy-1,2,3,4,5,8-hexamethylheme-substituted sperm whale Mb (6,7-dicarboxyheme-substituted Mb; Neya et al., 1998) shows substantial agreement between the two molecular models. The r.m.s.d. calculated over 153 $\text{C}\alpha$ pairs of the two Mb structures, crystallized in the space group P2_1 (this study) and in the space group P6 (Neya et al., 1998), respectively, is 0.56 \AA . Concerning the binding mode of cyanide to sperm whale Mb and to 6,7-dicarboxyheme-substituted Mb, quite satisfactory agreement between the coordination stereochemical parameters is observed (see Table 2). Nevertheless, 6,7-dicarboxyheme-substituted Mb displays a slightly shorter Fe-C coordination bond (1.89 \AA ; see Table 2) as compared to that of the sperm whale Mb:cyanide adduct here reported, and a significantly longer C-N bond length (1.25 \AA ; see Table 2), possibly reflecting the modified electronic structure of the 6,7-dicarboxyheme. The apparent decreased bond order within the cyanide (reflected by the $1.25\text{-}\text{\AA}$ C-N distance) may also result from restraints imposed during the crystallographic refinement or from partial disorder of the bound ligand. In this respect, it should be noted that a C-N distance of 1.31 \AA has been reported for the 5,10,15,20-tetramethylporphyrin-substituted sperm whale Mb:cyanide adduct (see Table 2; Neya et al., 1993).

Analysis of the Protein Data Bank archives of three-dimensional macromolecular structures (Abola et al., 1997) shows a substantial fluctuation in the coordination geometry of cyanide to monomeric hemoproteins (see Table 2). Although a comparison between hemoglobin structures refined at fairly different resolutions is achieved with difficulty, the inspection of Table 2 allows the following considerations.

Data reported in Table 2 indicate that the C-N covalent bond length is broadly clustered around three values, which are compatible with an undissociated HCN species (expected bond length 1.09 \AA), with a CN^- anionic species (expected bond length 1.15 \AA), and with a loosened bond order within the diatomic ligand or a partly disordered CN^- species (observed bond lengths $> 1.2 \text{ \AA}$) (Botschwina and Sebal, 1983; Jones et al., 1988). In this respect, among the

data here presented, the 100 K, 1.4-Å resolution structure of *L. pectinata* HbI:cyanide adduct, in consideration of the ligand binding stereochemistry and hydrogen bonding, is compatible with the presence of an unprotonated CN⁻ species. On the other hand, despite the differing C-N bond lengths observed in the refined (room temperature) structures of *L. pectinata* HbI and sperm whale Mb cyanide complexes (see Table 2), a less firm conclusion on the protonation state(s) of the ligand can be drawn, in view of the lower resolution achieved and the associated rms atomic coordinate errors.

Considering the heme iron coordination geometry (see Table 2), the Fe-C-N angle varies from 102°, in *C. caretta* Mb, to 177° in elephant Mb, indicating that the diatomic ligand orientation within the heme distal site may be dictated by the structural environment and by the nature of the interacting residues (Brancaccio et al., 1994; Springer et al., 1994; Bolognesi et al., 1997).

The Fe-C(cyanide) distance varies from 1.84 Å, in elephant Mb, to 2.54 Å in *L. pectinata* HbI (at room temperature; see Table 2). In this respect, the stereochemical arrangement of the ligand, observed in *L. pectinata* HbI at room temperature, may suggest 1) the (weak) electron donation of the cyanide π orbital to the heme iron d_{z^2} orbital (Busetto et al., 1977), or 2) the severe weakening (or cleavage) of the heme Fe-cyanide coordination bond, reflecting x-ray-induced Fe(III)→Fe(II) reduction, with concomitant drastic drop in the affinity for the ligand (see Bolognesi et al., 1997). On the contrary, reduction of the heme Fe(III) center may occur at a slower rate when the *L. pectinata* HbI:cyanide adduct crystals are exposed to a shorter wavelength source ($\lambda = 0.998$ Å) at cryogenic temperatures. In fact, x-ray absorption and the ensuing water radiolysis are wavelength dependent, with the shorter wavelengths showing significantly lower cross section. Moreover, cryofreezing of the crystals, before x-ray exposure, slows down the diffusion of free radicals from mother liquor to the Fe(III) center, allowing the collection of diffraction data of a virtually unperturbed ferric *L. pectinata* HbI:cyanide adduct.

In keeping with the reduction hypothesis, x-ray-induced Fe(III)→Fe(II) reduction has been shown to occur in cytochrome oxidase (Chance et al., 1980), in the heme-based NO carrier nitrophorin (Ding et al., 1999) and in other Fe-protein systems (Eriksson et al., 1988). Moreover, recent XANES studies on oxidized Cu, Zn superoxide dismutase have shown that reduction of the Cu(II) center occurs during x-ray irradiation, because of free radical species generated in the crystal solvent by x-ray-induced water radiolysis (Stroppolo et al., 1998). Thus (partial) reduction of the heme iron, related to x-ray exposure, to the wavelength of the incoming photons, and to the redox potential of the species under study, may be a relevant factor to be taken into account in the analysis of hemoprotein crystal structures.

This study was partially supported by grants from the Italian Ministry for University, Scientific Research and Technology (MURST, target-oriented project "Biocatalysis and Bioconversions"), from the Italian Space Agency (ASI, grant ARS-98-174), and from the Italian National Research Council (CNR, target-oriented project "Biotechnology").

REFERENCES

- Abola, E. E., J. L. Sussman, J. Prilusky, and N. O. Manning. 1997. Protein Data Bank archives of three-dimensional macromolecular structure. *Methods Enzymol.* 277:556–571.
- Bisig, D. A., E. E. Di Iorio, K. Diederichs, K. H. Winterhalter, and K. Piontek. 1995. Crystal structure of Asian elephant (*Elephas maximus*) cyanomet myoglobin at 1.78 Å resolution: Phe29(B10) accounts for its unusual ligand binding properties. *J. Biol. Chem.* 270:20754–20762.
- Bolognesi, M., D. Bordo, M. Rizzi, A. Tarricone, and P. Ascenzi. 1997. Nonvertebrate hemoglobins: structural bases for reactivity. *Prog. Biophys. Mol. Biol.* 67:29–68.
- Botschwina, P., and P. Sebal. 1983. Vibrational frequencies from anharmonic *ab initio* empirical potential energy functions: stretching vibration of hydrocyanic acid, isocyanacetilene and phosphabutadiene. *J. Mol. Spectrosc.* 100:1–23.
- Brancaccio, A., F. Cutruzzola, C. Travaglini Allocatelli, M. Brunori, S. J. Smerdon, A. J. Wilkinson, Y. Dou, D. Keenan, M. Ikeda-Saito, R. E. Brantley, Jr., and J. S. Olson. 1994. Structural factors governing azide and cyanide binding to mammalian metmyoglobins. *J. Biol. Chem.* 269:13843–13853.
- Busetto, C., A. D'Alfonso, F. Maspero, G. Perego, and A. Zazzetta. 1977. Side-on bonded dinitrogen and dioxygen complexes of rhodium(I): synthesis and crystal structures of *trans*-chloro(dinitrogen)-, chloro(dioxygen)-, and chloro(ethylene)-bis(tri-isopropylphosphine)rhodium(I). *J. Chem. Soc. Dalton Trans.* 1828–1834.
- CCP4. 1994. The CCP4 suite: programs for protein crystallography. *Acta Crystallogr.* D50:760–767.
- Chance, B., P. Angiolillo, and L. Powers. 1980. Identification and assay of synchrotron radiation-induced alterations on metalloenzymes and proteins. *FEBS Lett.* 112:178–182.
- Conti, E., C. Moser, M. Rizzi, A. Mattevi, C. Lionetti, A. Coda, P. Ascenzi, M. Brunori, and M. Bolognesi. 1993. X-ray crystal structure of *Aplysia limacina* myoglobin in different liganded states. *J. Mol. Biol.* 233:498–508.
- Ding, X. D., A. Weichsel, J. F. Andersen, T. K. Shokhireva, C. Balfour, A. Pierik, B. A. Averill, W. R. Montfort, and A. F. Walker. 1999. Nitric oxide binding to the ferri- and ferroheme states of nitrophorin 1, a reversible NO-binding heme protein from the saliva of the blood-sucking insect, *Rhodnius prolixus*. *J. Am. Chem. Soc.* 121:128–138.
- Eriksson, M., A. Jordan, and H. Eklund. 1988. Structure of *Salmonella typhimurium* *nrdF* ribonucleotide reductase in its oxidized and reduced forms. *Biochemistry.* 27:13359–13369.
- Evans, S. V., B. P. Sishta, A. G. Mauk, and G. D. Brayer. 1994. Three-dimensional structure of cyanomet-sulfmyoglobin C. *Proc. Natl. Acad. Sci. USA.* 91:4723–4726.
- Fukuyama, K., N. Kunishima, F. Amada, T. Kubota, and H. Matsubara. 1995. Crystal structures of cyanide- and triiodide-bound forms of *Arthromyces ramosus* peroxidase at different pH values. *J. Biol. Chem.* 270:21884–21892.
- Giardina, B., P. Ascenzi, M. E. Clementi, G. De Sanctis, M. Rizzi, and M. Coletta. 1996. Functional modulation by lactate of myoglobin: a monomeric allosteric hemoprotein. *J. Biol. Chem.* 271:16999–17001.
- Honzatko, R. B., W. A. Hendrickson, and W. E. Love. 1985. Refinement of a molecular model for lamprey hemoglobin from *Petromyzon marinus*. *J. Mol. Biol.* 184:147–164.
- Kraulis, P. J. 1991. MOLSCRIPT: a program to produce both detailed and schematic plots for protein structures. *J. Appl. Crystallogr.* 24:946–950.
- Kraus, D. W., and J. B. Wittenberg. 1990. Hemoglobins of the *Lucina pectinata*/bacteria symbiosis. I. Molecular properties, kinetics and equilibria of reactions with ligands. *J. Biol. Chem.* 265:16043–16053.
- Kraus, D. W., J. B. Wittenberg, L. Jing-Fen, and J. Peisach. 1990. Hemoglobins of the *Lucina pectinata*/bacteria symbiosis. II. An electron

We thank Prof. M. Brunori and Prof. L. Casella for reading the manuscript and providing constructive criticism. We are also grateful to Prof. A. Coda and Prof. M. Coletta for helpful discussions.

- paramagnetic resonance and optical spectral study of the ferric proteins. *J. Biol. Chem.* 265:16054–16059.
- Kuranova, I. P., A. V. Teplyakov, G. V. Obmolova, A. A. Voronova, A. N. Popov, D. M. Kheiker, and E. H. Harutyunyan. 1982. X-ray diffraction study of leghemoglobin in complexes with nitrosobenzene, nicotinic acid and acetate, fluoride and cyanide ions. *Bioorg. Khim.* 8:1625–1636.
- Jones, P. G., H. W. Roesky, and J. Schimkowiak. 1988. How do silver(I) cations react with hydrogen cyanide? The crystal structure of $[\text{Ag}(\text{NCH})_2][\text{SbF}_6]$. *J. Chem. Soc. Chem. Commun.* 730.
- Jones, T. A., S. W. Cowan, and M. Kjeldgaard. 1991. Improved methods for building protein models in electron density maps and the location of errors in these models. *Acta Crystallogr.* A47:110–119.
- Leslie, A. G. W. 1992. Joint CCP4 and ESF-EACBM. *Newslett. Protein Crystallogr.* No. 26. SERC Daresbury Laboratory, Warrington, UK.
- Lionetti, C., M. G. Guanziroli, F. Frigerio, P. Ascenzi, and M. Bolognesi. 1991. X-ray crystal structure of the ferric sperm whale myoglobin: imidazole complex at 2.0 Å resolution. *J. Mol. Biol.* 217:409–412.
- Nardini, M., C. Tarricone, M. Rizzi, A. Lania, A. Desideri, G. De Sanctis, M. Coletta, R. Petruzzelli, P. Ascenzi, A. Coda, and M. Bolognesi. 1995. Reptile heme protein structure: x-ray crystallographic study of the aquomet and cyano-met derivatives of the loggerhead sea turtle (*Caretta caretta*) myoglobin at 2.0 Å resolution. *J. Mol. Biol.* 247:459–465.
- Neya, S., N. Funasaki, N. Igarashi, A. Ikezaki, T. Sato, K. Imai, and N. Tanaka. 1998. Structure and function of 6,7-dicarboxyheme-substituted myoglobin. *Biochemistry.* 37:5487–5493.
- Neya, S., N. Funasaki, T. Sato, N. Igarashi, and N. Tanaka. 1993. Structural analysis of the myoglobin reconstituted with iron porphyrin. *J. Biol. Chem.* 268:8935–8942.
- Nguyen, B. D., X. Zhao, K. Vyas, G. N. L. La Mar, R. A. Lile, E. A. Brucker, G. N. Phillips, Jr., J. S. Olson, and J. B. Wittenberg. 1998. Solution and crystal structures of a sperm whale triple mutant that mimics the sulfide-binding hemoglobin from *Lucina pectinata*. *J. Biol. Chem.* 273:9517–9526.
- Orpen, A. G., L. Brammer, F. H. Allen, O. Kennard, D. Watson, and R. Taylor. 1989. Tables of bond lengths determined by x-ray and neutron diffraction. 2. Organometallic compounds and co-ordination complexes of the d- and f-block metals. *J. Chem Soc. Dalton Trans.* S1–S83.
- Paoli, M., G. Dodson, R. C. Liddington, and A. J. Wilkinson. 1997. Tension in haemoglobin revealed by Fe-His(F8) bond rupture in the fully liganded T-state. *J. Mol. Biol.* 271:161–167.
- Perutz, M. F. 1979. Regulation of oxygen affinity of hemoglobin: influence of structure of the globin on the heme iron. *Annu. Rev. Biochem.* 48:327–386.
- Read, R. J. 1986. Improved Fourier coefficients for maps using phases from partial structures with errors. *Acta Crystallogr.* A42:140–149.
- Rizzi, M., J. B. Wittenberg, A. Coda, P. Ascenzi, and M. Bolognesi. 1996. Structural bases for sulfide recognition in *Lucina pectinata* hemoglobin I. *J. Mol. Biol.* 258:1–5.
- Rizzi, M., J. B. Wittenberg, A. Coda, N. Fasano, P. Ascenzi, and M. Bolognesi. 1994. Structure of the sulfide reactive hemoglobin from the clam *Lucina pectinata*: crystallographic analysis at 1.5 Å resolution. *J. Mol. Biol.* 244:86–99.
- Schlichting, I., J. Berendzen, G. N. Phillips, Jr., and R. M. Sweet. 1994. Crystal structure of photolyzed carbonmonoxy-myoglobin. *Nature.* 371:808–812.
- Sheldrick, G. M., and T. R. Schneider. 1997. SHELXL: high-resolution refinement. *Methods Enzymol.* 277:319–343.
- Springer, B. A., S. G. Sligar, J. S. Olson, and J. N. Phillips, Jr. 1994. Mechanisms of ligand recognition in myoglobin. *Chem. Rev.* 94:699–714.
- Steigemann, W., and E. Weber. 1979. Structure of erythrocrucorin in different ligand states refined at 1.4 Å resolution. *J. Mol. Biol.* 127:309–338.
- Stroppolo, M. E., S. Nuzzo, A. Pesce, C. Rosano, A. Battistoni, M. Bolognesi, S. Mobilio, and A. Desideri. 1998. On the coordination and oxidation states of the active-site copper ion in prokaryotic Cu, Zn superoxide dismutases. *Biochem. Biophys. Res. Commun.* 249:579–582.
- Takano, T. 1977. Structure of myoglobin refined at 2.0 Å resolution: crystallographic refinement of metmyoglobin from sperm whale. *J. Mol. Biol.* 110:537–568.
- Teng, T. Y., V. Srajer, and K. Moffat. 1994. Photolysis-induced structural changes in single crystals of carbonmonoxy myoglobin at 40 K. *Nature Struct. Biol.* 1:701–705.
- Tronrud, D. E., L. F. Ten Eyck, and B. W. Matthews. 1987. An efficient general purpose least-squares refinement program for macromolecular structures. *Acta Crystallogr.* A43:489–501.
- Weichsel, A., J. F. Andersen, D. E. Champagne, F. A. Walker, and W. R. Montfort. 1998. Crystal structure of a nitric oxide transport protein from a blood-sucking insect. *Nature Struct. Biol.* 5:304–309.
- Wittenberg, J. B., and B. A. Wittenberg. 1990. Mechanisms of cytoplasmic hemoglobin and myoglobin function. *Annu. Rev. Biophys. Biophys. Chem.* 19:217–241.